Article

A high resolution study of dynamic changes of Ce2O3 and CeO2 nanoparticles in complex environmental media

Ruth Corrin Merrifield, Kenton P. Arkill, Richard E. Palmer, and Jamie R Lead

Environ. Sci. Technol., **Just Accepted Manuscript** • DOI: 10.1021/acs.est.7b01130 • Publication Date (Web): 15 Jun 2017

A high resolution study of dynamic changes of Ce_2O_3 and CeO_2 nanoparticles in complex environmental media

Ruth C. Merrifield,[1, 2], Kenton P. Arkill[3, 4], Richard E. Palmer[5], [*]Jamie R. Lead[1, 2]

[1] Department of Geography, Earth and Environmental sciences, University of Birmingham, Birmingham, UK
[2] Center for Environmental Nanoscience and Risk, University of South Carolina, Columbia, SC, USA
[3] School of Medicine, University of Nottingham, Nottingham, UK
[4] CSIC UPV/EHU and PiE, University of the Basque Country, Spain
[5] Nanoscale Physics Research Laboratory, Physics and Astronomy, University of Birmingham, Birmingham, UK

18 TOC art

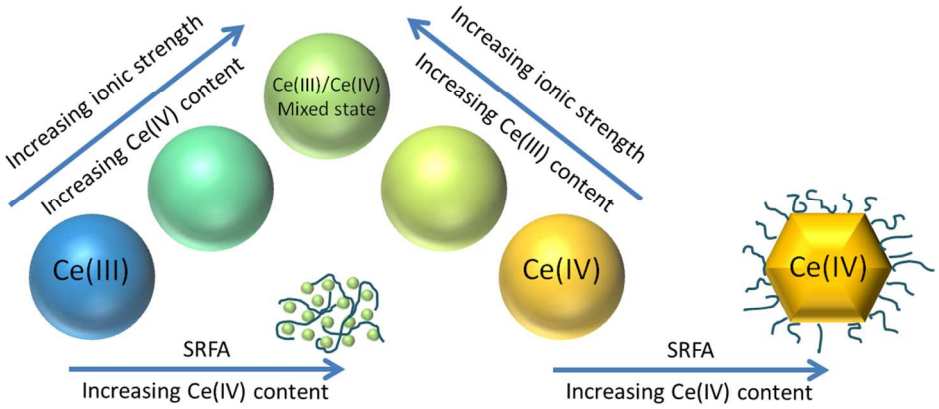
Increasing ionic strength
Increasing Ce(IV) content
Ce(III)/Ce(IV)
Mixed state
Increasing ionic strength
Increasing Ce(III) content
Ce(III)
Ce(IV)
Ce(IV)
SRFA
Increasing Ce(IV) content
SRFA
Increasing Ce(IV) content

19

ABSTRACT

Ceria nanoparticles (NPs) rapidly and easily cycle between Ce(III) and Ce(IV) oxidation states, making them prime candidates for commercial and other applications. Increased commercial use has resulted in increased discharge to the environment and increased associated risk. Once in complex media such as environmental waters or toxicology exposure media, the same redox transformations can occur, causing altered behavior and effects compared to the pristine NPs. This study used high resolution scanning transmission electron microscopy and electron energy loss spectroscopy to investigate changes in structure and oxidation state of small, polymer-coated ceria suspensions in complex media. NPs initially in either the III or IV oxidation states, but otherwise identical, were used. Ce(IV) NPs were changed to mixed (III, IV) NPs at high ionic strengths, while the presence of natural organic macromolecules (NOM) stabilized the oxidation state and increased crystallinity. The Ce(III) NPs remained as Ce(III) at high ionic strengths, but were modified by the presence of NOM, causing reduced crystallinity and degradation of the NPs. Subtle changes to NP properties upon addition to environmental or ecotoxicology media suggest that there may be small but important effects on fate and effects of NPs compared to their pristine form.

INTRODUCTION

Interactions and transformations of NPs with environmental and toxicological media are known to occur[1-3] but are often not well studied, although published work focuses on changes in dissolution, aggregation, shape, size and size distribution[3]. In the case of ceria NPs that do not readily dissolve in water but can transform chemically[4], transformations such as Ce(III) to Ce(IV) cycling and associated changes are likely to be of key importance for understanding biological and environmental behavior.[5] These same chemical transformations make ceria NPs of particular interest to industry, in particular they are widely used in microelectronics/semi-conductor industries, as mechanical polishers, [6-9] and as a fuel additive in diesel.[10, 11] The oxidation state of ceria NPs is known to be size dependent [12, 13] with the larger particles preferentially in the tetravalent (Ce(IV)) state and smaller NPs preferentially in the trivalent (Ce(III)) state. However, particles can easily cycle between the trivalent and tetravalent states of Ce,[14] with implications for biological behavior such as the production of reactive oxygen species (ROS) and oxidative stress. A number of ceria NP types have been shown to have an anti- or pro-oxidant effect, but these potentially protective properties are strongly dependent on the surrounding buffer composition and pH [15], while polymer coatings can reduce the toxic effects of the NPs [16]. The toxicity of ceria NPs reported in the literature is inconclusive with both low [17] and higher [18] toxicities reported. Differences are possibly linked to morphological changes or surface oxidation state, which themselves have been linked to high toxicity via the production of ROS[12]. Some studies have also shown that redox behavior can impact dissolution; although ceria is believed to have a low solubility, in some cases ionic Ce from dissolution has been shown to be sufficient to explain some toxicity [19] .

One key aspect in understanding and then predicting the likely environmental toxicity and behaviors of ceria NPs is their redox (and crystallinity) changes and how this is affected by environmental and toxicology exposure media. This study aims to observe the effect of ionic strength and NOM from representative toxicology exposure and environmental media on the structure and oxidation state of two small, PVP capped ceria NPs. The results will increase understanding in processes such as toxicity and environmental transport.

MATERIALS AND METHODS

Nanoparticle synthesis. Cerium(III) oxide NPs, nominally 5 nm, were synthesized and characterized as previously published [4]. Briefly, Ce(III)NO_3 (Sigma Aldrich) was dissolved in a solution of 10 KDa polyvinylpyrrolidone (PVP, Sigma Aldrich). The mixture was heated for 3 hours at 105 °C, followed by quenching the flask into cold water. When the reaction mixture was cooled, the excess PVP was removed by adding acetone, centrifuging at 4000 rpm for 10 minutes using an Eppendorf 5810R bench top centrifuge. The yellow pellet was retained, and the excess liquid was discarded. The pellet was resuspended in ultrahigh purity water (UHP, resistivity 18.2 MΩ cm, total organic carbon <10 ppb). This procedure was repeated three times to ensure all excess PVP was removed. After the final resuspension in UHP water, the NPs were re-dispersed to 100 ml of UHP water and filtered through a 100 nm mixed cellulose ester membrane (EMD Millipore™) filter using an asepic vacuum filter system (EMD Millipore™) to a selected concentration and stored at room temperature in the dark.

Cerium (IV) oxide NPs were produced by converting 50 mL of cerium (III) stock NP suspension. 50ml of the Ce_2O_3 NP suspension was placed into a 125 mL Teflon-lined autoclave with 1ml of 1M NaOH and heated at 140 °C for 4 hours. The resulting solution turned bright orange and contained CeO_2 NPs. The suspension was ultrafiltered using an Amicon™ stirred ultrafiltration cell (EMD Millipore™) and a 3 KDa Ultracel™ ultrifiltration disc, made from regenerated cellulose (EDM Millipore™), to remove any excess cerium ions and unreacted NaOH. Finally the suspension was filtered through a 100 nm mixed cellulose ester membrane (Millipore) filter using a vacuum filter system (Millipore) to remove any aggregated particles and stored under the same conditions as the Ce(III) oxide NPs.

Preparation of Ceria NPs in media. The two NP suspensions were separately added to four different environmental conditions including OECD and ISO algae and daphnia media and a synthetic EPA soft water, and synthetic EPA soft water with 8 mg L^{-1} of Suwanee River fulvic acid (SRFA). A full list of conditions, sample abbreviations and their compositions are given in S1 (Table S1-A and S1-B). The particle solutions were left for 72 hours, equivalent to toxicological exposure conditions for algae[20], and relevant to environmental exposures. Suspensions of 100 ppb were prepared in each media and left under ambient laboratory conditions for 72 hours. Aliquots were withdrawn at 0, 24, 48 and 72 hours for testing. All experiments performed in triplicate. The suspension was not shaken after mixing and no particle precipitation was observed.

Characterization. Measurements were performed on a Malvern Instruments Nanosizer to collect both size and zeta potential data. For the size measurements 1 ml of particle suspension was placed into a polystyrene disposable cuvette (Sarstedt AG &Co.). Ten consecutive measurements were collected and averaged to calculate a Z average size. The results were taken at 20 °C with samples equilibrated for 2 min before measurements were started. The Stokes relationship was used to calculate the hydrodynamic diameter of the particles. For the zeta potential measurements 1 ml of suspension was put into a disposable folded capillary cell (Malvern Instruments Ltd.). The sample was allowed to equilibrate at 20 °C for 2 minutes before five consecutive measurements were made.

Flow field flow fractionation (FlFFF), high-angle annular dark-field scanning transmission electron microscopy (HAADF-STEM) and electron energy loss spectroscopy (EELS) were

also used to examine the NPs. FlFFF separation and sizing were carried out on a Postnova asymmetrical field-flow fractionation (AF2000 Mid Temperature, Postnova Analytic). The accumulation wall was a 1 KDa regenerated cellulose membrane. The eluent was 0.01 M NaCl (pH 7.5). The channel flow was 1 mL min^{-1} and cross-flow was 2 mL min^{-1}, to ensure a good separation between the void peak and particle elution time. The injection volume was 0.5 mL (particle concentration of approximately 100 ppb), which was injected into the channel after 6 min. The channel volume was calculated using 20, 30, and 60 nm polystyrene bead standards (Duke Scientific Corp.). All particles were detected with a UV detector at 254 nm. Diffusion coefficients were calculated using FlFFF theory[21] and converted to size using the Stokes relationship. At least 3 replicates were collected and a mean size calculated.

Samples for HAADF-STEM analysis were prepared by placing an amorphous carbon coated copper grid (Agar Scientific, UK) onto a bespoke Teflon flat surface in a 12ml ultracentrifugation tube as we have previously preformed[22]. 11 ml of NP suspension was placed into the tube and centrifuged at 500,000 g for 1 hour using a Beckman ultracentrifuge (L7-65 Ultracentrifuge) with a swing out rotor (SW40Ti) on to a carbon coated copper TEM grid. The supernatant, containing the ionic fraction of the suspension, was removed and discarded while the grid was recovered and washed by carefully placing into UHP water for 5 minutes. The grid was removed from the wash water and allowed to fully dry at room temperature for at least two hours before imaging. The maximum time between grid preparation and imaging was kept to below 12 hours.

HAADF-STEM and EELS data were obtained at 200 KeV on a Jeol 2100F coupled with a CEOS spherical aberration probe corrector and a Gatan Enfina EELS. The STEM images were used to analyze and compare NP morphology within the samples. The STEM probe size is circa 0.1 nm. The lattice spacing for each suspension were measured using Digital Micrograph software by taking line profiles across the (111) lattice direction on the HAADF-STEM micrographs. Lattice spacings were measured for at least 30 NPs in each suspension. A student t-test was performed between all lattice spacing sets (NPs as prepared and in media) to calculate any significant changes after addition to exposure media.

The oxidation state of the NPs was investigated using EELs. The spatial resolution of the EELS is comparable to that of the STEM probe (0.1 nm) and the energy resolution in the order of 1 eV. Pixel sizes of 0.065 – 1 nm were used in recording one-dimensional EELS spectra, dependent on the particle size. Cerium oxidation state is sensitive to the electron beam with prolonged beam time. To minimize this damage the total time over a single point was kept to 3 seconds, as performed previously.[23] Line acquisitions took three 1 s spectra for each point along the line and the mean calculated [4, 24].

The EELS spectra of cerium is characterized by two sharp edges at 903 eV (M4 edge) and 886 eV (M5 edge) that are due to the transition of a core electron to an unbound state, 3d3/2→4f5/2 and the 3d5/2→4f7/2, respectively (An in depth discussion of the EELS analysis can be found in a previous paper Merrifield et al 2013[4]). There are many different methods employed to analyze the EELS spectra to obtain the Ce(III):Ce(IV) ratio[25] but here the second derivative method was used, as this has been shown to be less susceptible to alterations in sample

thickness [26]. The integrated intensity of each edge was calculated between the points of inflection in the second derivative to find the ratio between the M5 and M4 edge. The raw EELS signal was background corrected, low pass filtered, and the second derivative calculated using the digital micrograph software. The M5/M4 ratio was then determined using the integrated intensities of the peaks in the second derivative.

The relative positions, intensities and shapes of the M4 and M5 edges present in the EELS spectra differently for the Ce(III) and Ce(IV) spectra[4]. In comparison to the Ce(III) signal the edges in the Ce(IV) spectra are shifted to a slightly higher energy and a shoulder appears to on the M4 edge [27]. The ratio of the edge maximum intensities also alters. The ratios of these peaks (M5/M4) can vary somewhat in the literature and have been quoted to be anywhere between 0.79-0.91 and 1.11-1.31 for Ce(IV) and Ce(III) respectively[4, 13, 28] showing the importance of calibrating to a known standard. In this work, an M5/M4 ratio of 0.80 (±0.1) and 1.23 (±0.15) were obtained for Ce(IV) and Ce(III) standards, respectively[4].

177 **RESULTS AND DISCUSSION**

178

179 The hydrodynamic diameter data (measured by DLS and FIFFF) and electrophoretic mobility
180 (EPM) of particles in exposure media at time 0 and 72 h are summarized in Table 1 (data in
181 supporting information Figures S2A and B). All of the suspensions, with the exception of one,
182 had hydrodynamic diameters of in the range 6-9 nm and there was no significant difference
183 between the as-prepared NPs and the NPs in media. However, the Ce(III) NPs in soft water
184 containing SRFA gave an immediate increase in hydrodynamic diameter to > 120 nm, which
185 was substantially different from the as-prepared size of 6.2 ± 0.1 nm. This increase was
186 significantly different from all of the other suspensions ($p << 0.05$). Interestingly, the FIFFF
187 measurements showed no significant differences in any of the sizes ($p > 0.05$), including
188 Ce(III) in soft water with SRFA. However the intensity data for these NPs was less than 50%
189 of the other conditions, indicating losses, most likely due to aggregation, as we have seen
190 before[3]. The combination of the two methods allowed improved identification of
191 transformation: Ce(III) NPs in soft water containing SRFA underwent some aggregation, based
192 on DLS data which is biased towards larger particles and loss of peak signal in FFF, with over
193 50% of the initial mass present in the aggregates and slightly under 50% remaining as the
194 original dispersed NPs (from intensity data). Likely this agglomeration was from a mixture of
195 the starting components: mixtures of FA, partly degraded ceria NPs and cerium ions. This
196 assumption is supported by the STEM-EELS data provided later. Changes in electrophoretic
197 mobility were also measured upon addition into the media. Certain general observations were
198 clear: Firstly Ce(IV) NPs were always negatively charged and showed no temporal changes.
199 Secondly for both NPs, the electrophoretic mobility appears to be controlled by FA if present,

as expected[29, 30], and showed no temporal changes, suggesting interactions were rapid compared to the measurement time. In addition, Ce (III) NPs showed some significant temporal changes in the Daphnia media and softwater, which were broadly comparable and composed of only major ions, lacking the transition metals or FA present in the other media (Figure S3). Previously, we have seen no effect on PVP aggregation with ionic strength,[31] although we have seen alterations in some PVP behavior with increasing ion concentrations.[32] Speculatively, the increased ionic strength or specific ion concentration affects the polymer chemistry, possibly affecting the nature of the core redox behavior.

HAADF-STEM and EELs were utilized to investigate potentially subtle changes in morphology and oxidation state of synthesized Ce(III) and Ce(IV) NPs after exposure to standard ecotoxicology and synthetic environmental media. Figure 1 shows a typical HAADF-STEM image for the Ce(III)-stock, Ce(IV)-stock, Ce(III)-softwater with fulvic acid and Ce(IV)-softwater with fulvic acid after 72 h in the suspension. All the other particles in the algae, daphnia and softwater media suspensions showed no observable morphological differences from the stock suspensions so were not included. The Ce(III)-softwater with SRFA NPs have less ordered structure than the Ce(III)-stock suspension. Although some smaller particles were present (depicted in Figure 1) in the softwater medium, there were also larger, unstructured materials (shown in Figure S4). These were not observed in any other suspensions. The HAADF-STEM images agreed with the previously shown DLS and FIFFF data, indicating that the presence of SRFA in these media resulted in alterations, including formation of loosely bound agglomerates of partially degraded ceria NPs and FA. The changes observed were not seen in other NPs in this study or in PVP stabilized NPs with other core

materials[31]), suggesting that media-induced transformations are dependent on core material, as well as coating and media conditions. The (111) lattice spacing for the Ce(III)-stock and Ce(IV)-stock NPs were measured as 0.34 (±0.09) and 0.32 (±0.01), very similar to literature data[13]). These values did not change significantly for any of any NPs in any media, with the exception of the Ce(III)-softwater with fulvic acid suspension, where no measurement was possible due to aggregation.

The oxidation state of the NPs was investigated using EELs. Both spatially averaged and spatially resolved data was recorded. The M5/M4 was used to derive oxidation state ratio with reference Ce(III) and Ce(IV) measured as 1.23 (± 0.15) and 0.80 (± 0.10) respectively[4], in agreement with data in the literature [4, 33]. Figures in brackets are standard deviations. These values were used to assess the oxidation state of the NPs as prepared and in the various media. The mean oxidation state for each suspension was measured by comparing the ratio of the M5/M4 peaks in the EELs spectra as described in the literature[4]. As expected there is a significant difference between the Ce(III)-stock and Ce(IV)-stock suspensions with $p < 0.05$ showing that initially the particles were in different oxidation states.

The M5/M4 ratios for the different suspensions of originally Ce(III) after 72 h can be seen in Figure 2 (Raw data can be found in Figure S5). T-tests were performed, primarily with the aim of identifying any changes in oxidation state due to the exposure to different media types compared with the same NPs in the stock. (A table of p values can be found in Table S6). For Ce(III) NPs, significant changes occurred after spiking into the algal and daphnia exposure media, but not into the soft water either with or without SRFA. It should be noted first that the

Ce(III)-softwater with SRFA has a larger error related to the aggregation and amorphous nature of the particles making accurate quantification difficult and, secondly, that these significant differences were small in magnitude. The origin of these changes is not clear, with the primary difference in the medium being the higher ionic strength of the exposure media compared to the soft water. The greater complexity of the algal media containing redox active transition metals plays no obvious role. However, the changes are small not significant, with the exception of the dramatic effect of the SRFA on Ce(III). It is likely if there is a redox effect due to the SRFA causing oxidation and (partial) dissolution of the ceria NP, possibly enhancing polymer bridging[34] between PVP and hence forming weakly bound agglomerates. This interaction is in contrast to the lack of interaction with PVP on gold NPs measured using different methods[31] , suggesting a combined effect of core transformations disruption of the PVP coating and ceria, cerium and SRFA interaction to form loosely bound agglomerates.

In the case of Ce(IV) NPs a significant ($p < 0.05$) and larger change in oxidation state was observed upon spiking NPs into the algal and daphnia media, but there was no corresponding change in EPA softwater either with or without SRFA. Semi-quantitatively, the reduction was between 0-50%, dependent on new media (Figure 2; Table S7), although there was some spatial variability between and within single particles. The relatively simple composition of daphnia media suggests that the high ionic strength and presence of specific ions rather than the presence of transition metals affect redox behavior. Most likely, the interactions of ions with the PVP caused an indirect effect on the ceria core redox behavior, although the exact mechanism is not clear. Taking Figures 1 and 2 together, the SRFA media reduces transformations of the Ce(IV) NPs, while the lower ionic strength media has little effect. The

diametrically opposite behavior of FA with Ce(III) and Ce(IV) is noteworthy, given the different likely behaviors of these NPs to identical solution conditions.

Examples of spatially resolved HAADF-STEM-EELS data on individual NPs are shown in Figure 3. Examples for Ce(IV)-stock, Ce(IV)-algae and Ce(IV)-softwater with fulvic acid micrographs are shown with corresponding M5/M4 ratios along a radial profile. In the Ce(IV)-stock and Ce(IV)-softwater with fulvic acid case the M5/M4 ratio remains consistently close to 0.8 from the center to the edge of the particles. Interestingly, the NPs in the SRFA containing media show a more consistent pattern with no change. However, in the stock, there is an indication the M5/M4 ratio increases towards the edge, showing a greater degree of Ce(III) character at the edge as would be expected[35]. This result highlights the stability of the Ce(IV) oxidation state in these samples, particularly in the presence of SRFA. In contrast, in the Ce(IV) NPs in algal media, there is a variation in M5/M4 ratio throughout the particle. These changes appear to be random, but do indicate a change from a predominantly Ce(IV) oxidation state at the core of the particle to a mixed (III, IV) state. Again, there is an indication that the oxidation state becomes predominantly Ce(III) at the edge. It is generally accepted that the Ce(III) oxidation state is more energetically favorable for small cerium NPs [36], agreeing with our data. In the absence of the protective SRFA, the tendency might be for these NPs to become dominated by the Ce(III) state. There have been discussions in the (eco)toxicology community regarding the use of dispersants and whether or not to use natural organic macromolecules (NOM) as a 'natural dispersant' to overcome aggregation and other transformations[37]. The data here suggests that, for Ce-containing NPs and perhaps other similar NPs, NOM may be useful in controlling transformations. However, in certain cases such as the

292 ceria (III) NPs, NOM may also enhance transformations. In spite of this, NOM additions may
293 be useful since they lead to conditions which more closely resemble exposure conditions in the
294 environment.
295
296 The observed results have important implications for the fate and behavior, bioavailability and
297 toxicology of ceria NPs. The high resolution physical and chemical characterization of NP
298 dynamics has been essential in obtaining data on these subtle changes in NP in media relevant
299 to ecotoxicology exposures and media. In particular, exposure of NPs to inorganic standard
300 exposure media leads to small but potentially significant changes in NP oxidation state. The
301 role of NOM such as SRFA is more pronounced but causes very different transformational
302 behaviors depending on the starting NP, with Ce(III) NPs changing and agglomerating, while
303 Ce(IV) NPs appear to be stabilized and transformations minimized. This, and similar high
304 resolution TEM-EELS studies on silver NPs[24, 38], need to be incorporated in future research to
305 understand better the full extent of these subtle transformations, which can then be linked
306 mechanistically to transport and bioavailability studies.
307

308 FIGURES

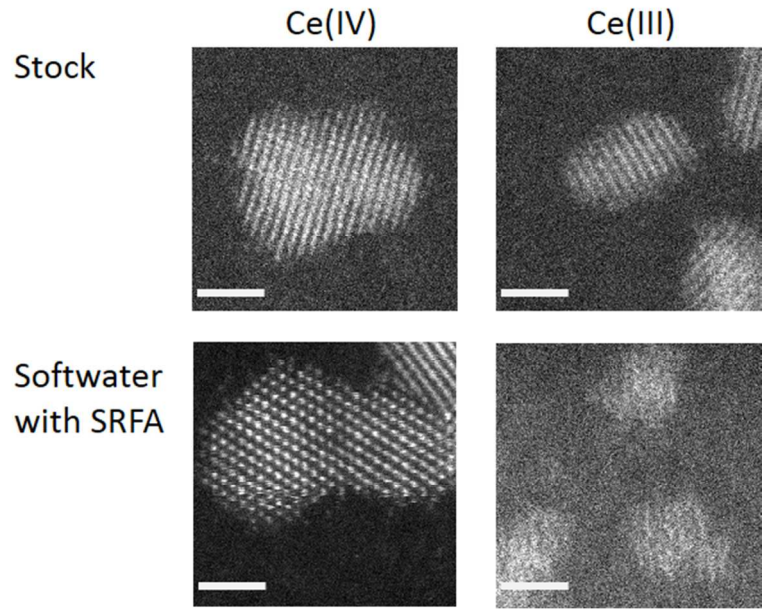

309

310 Figure 1: Typical STEM images of Ce(IV)-stock, Ce(III)-stock, Ce(IV)-softwater with SRFA

311 and Ce(III)-softwater with SRFA. The bars in the image are 2 nm.

312

313

314

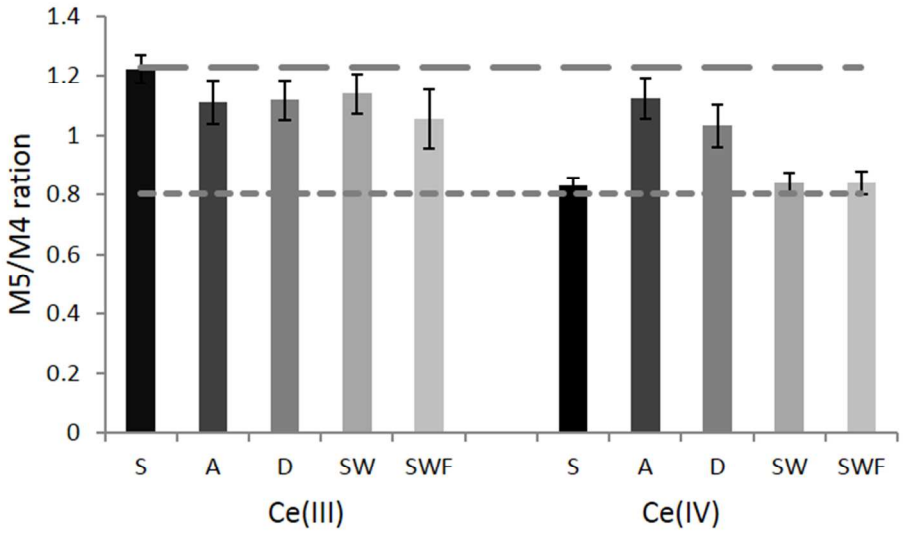

315

316 Figure 2: The average ratios of the M5/ M4 cerium peaks from EELs spectrum for the centre of
317 the particles when exposed to different media. The dashed line is the expected ratio for pure
318 Ce(III) (1.23) , the dotted line is the ratio for pure Ce(IV) (0.802). S - stock; A –algal media; D
319 – daphnia media; SW – soft water; SWF – soft water with SRF

320

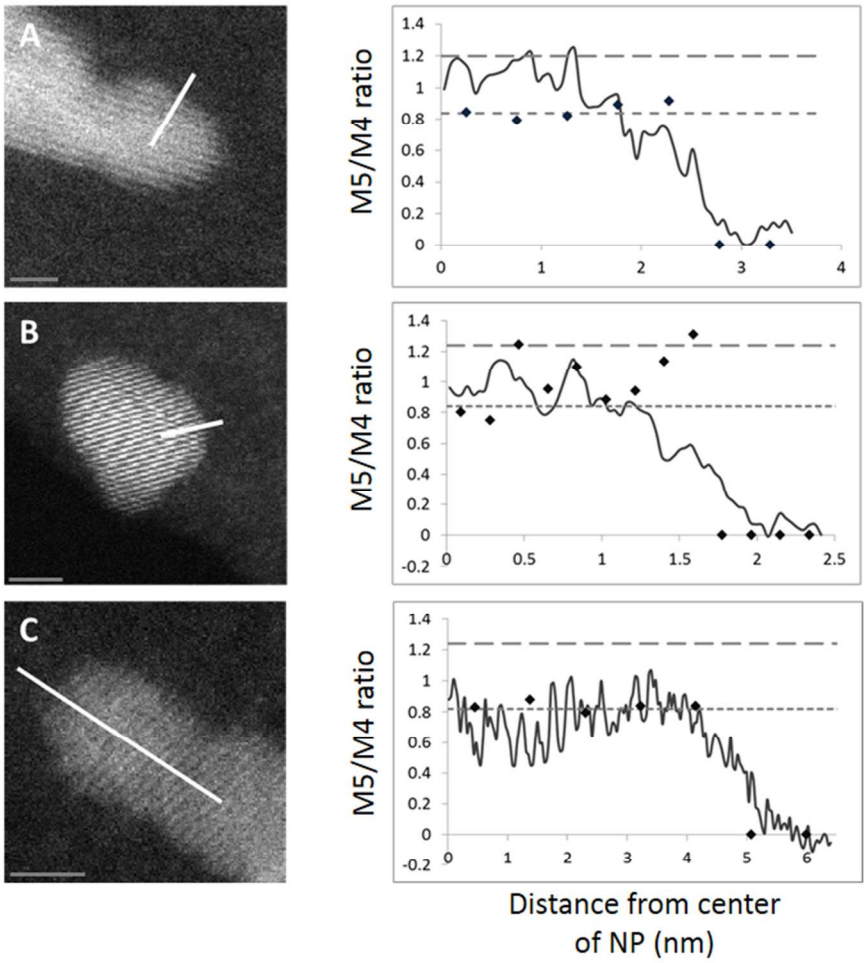

Figure 3. HAADF-STEM micrographs with corresponding spatially resolved EELs analysis. Line intensity profiles (solid dark gray line) were taken from the corresponding lines (white) on the HAADF-STEM micrographs with corresponding M5/M4 ratios from the EELS analysis (black diamonds) for three suspensions A) Ce(IV)-stock, B) Ce(IV)-algae, and Ce(IV)-softwater with SRFA NPs from suspension. The M5/M4 ratios for Ce(III) and Ce(IV) reference samples are shown by the light grey dashed and dotted horizontal lines respectively. Scale bars are 2 nm shown in grey on the images.

331 TABLES.

	DLS				Zeta				FFF			
	0 hours		72 hours		0 hours		72 hours		0 hours		72 hours	
	Size (nm)	PDI	Size (nm)	PDI		SD		SD	Size (nm)	SD	Size (nm)	SD
Ce(III)S	6.2	0.13	6.2	0.13	0.43	0.15	0.43	0.15	7.43	2.15		
Ce(III)A	8.6	0.4	7.5	0.3	-10.15	0.69	-7.3	1.96	6.58	1.14	7.26	1.23
Ce(III)D	6.6	0.8	7.3	0.3	10.47	0.56	-2.66	1.45	7.20	1.11	7.29	1.15
Ce(III)SW	7.9	0.5	7.2	1.0	8.60	0.63	-6.36	0.33	6.50	0.84	6.71	1.26
Ce(III)SWF	122.8	0.3	122.6	0.3	-14.10	1.13	-15.70	0.14	8.05	1.15	7.65	1.08
Ce(IV)S	6.9	0.2	6.9	0.2	-17.20	0.95	-17.20	0.95	6.90	1.13		
Ce(IV)A	7.9	0.5	7.8	0.4	-23.20	1.27	-19.22	1.71	7.02	1.16	7.50	1.17
Ce(IV)D	8.1	0.7	8.5	0.1	-4.04	1.31	-7.62	1.54	7.16	1.14	7.49	1.17
Ce(IV)SW	7.6	0.5	8.3	0.6	-14.40	1.52	-14.71	0.71	7.68	1.12	7.75	1.12
Ce(IV)SWF	8.4	0.7	8.8	0.8	-12.40	3.15	-14.80	0.99	7.25	1.04	7.26	1.06

332

333 Table 1. Hydrodynamic diameters (measured by FIFFF and DLS) and surface potential
334 (measured by Zeta potential) of NP suspensions in different media at time 0 and 72 hours
335 (Please refer to the key in S1-A for annotation names).

336
337
338
339
340
341
342
343
344
345
346
347
348
349

Supporting information is provided on sample information, media contents, DLS results, FIFFF results, Z-potential results, further STEM image of $Ce(III)_{SWF}$ NPs, Ce(III) and Ce(IV) standards for EELS and original M5/M4 ratio data. This material is available free of charge via the Internet at http://pubs.acs.org.

355 AUTHOR INFORMATION

356 **Corresponding Author**

357 * Prof. Jamie R. Lead. JLEAD@mailbox.sc.edu.

358 **Author Contributions**

359 The manuscript was written through contributions of all authors. All authors have given
360 approval to the final version of the manuscript.

361

362 **Funding Sources**

363 The authors acknowledge the SmartState CENR, the NERC (NE/H013148/1; NanoBEE;
364 FENAC) and the Science City Research Alliance (UK)

365

References

1. Lowry, G. V.; Gregory, K. B.; Apte, S. C.; Lead, J. R., Transformations of Nanomaterials in the Environment. *Environmental Science & Technology* **2012,** *46*, (13), 6893-6899.
2. Romer, I.; Gavin, A. J.; White, T. A.; Merrifield, R. C.; Chipman, J. K.; Viant, M. R.; Lead, J. R., The critical importance of defined media conditions in Daphnia magna nanotoxicity studies. *Toxicol. Lett.* **2013,** *223*, (1), 103-108.
3. Romer, I.; White, T. A.; Baalousha, M.; Chipman, K.; Viant, M. R.; Lead, J. R., Aggregation and dispersion of silver nanoparticles in exposure media for aquatic toxicity tests. *J. Chromatogr. A* **2011,** *1218*, (27), 4226-4233.
4. Merrifield, R. C.; Wang, Z. W.; Palmer, R. E.; Lead, J. R., Synthesis and characterization of polyvinylpyrrolidone coated cerium oxide nanoparticles. *Environmental science & technology* **2013,** *47*, (21), 12426-33.
5. Graham, U. M.; Tseng, M. T.; Jasinski, J. B.; Yokel, R. A.; Unrine, J. M.; Davis, B. H.; Dozier, A. K.; Hardas, S. S.; Sultana, R.; Grulke, E. A.; Butterfield, D. A., In Vivo Processing of Ceria Nanoparticles inside Liver: Impact on Free-Radical Scavenging Activity and Oxidative Stress. *Chempluschem* **2014,** *79*, (8), 1083-1088.
6. Zantye, P. B.; Kumar, A.; Sikder, A. K., Chemical mechanical planarization for microelectronics applications. *Materials Science & Engineering R-Reports* **2004,** *45*, (3-6), 89-220.
7. Cumbo, M. J.; Fairhurst, D.; Jacobs, S. D.; Puchebner, B. E., Slurry particle size evolution during the polishing of optical glass. *Appl. Opt.* **1995,** *34*, (19), 3743-3755.
8. Hoshino, T.; Kurata, Y.; Terasaki, Y.; Susa, K., Mechanism of polishing of SiO2 films by CeO2 particles. *Journal of Non-Crystalline Solids* **2001,** *283*, (1-3), 129-136.
9. Stanek, C. R.; Tan, A. H. H.; Owens, S. L.; Grimes, R. W., Atomistic simulation of CeO(2) surface hydroxylation: implications for glass polishing. *Journal of Materials Science* **2008,** *43*, (12), 4157-4162.
10. Sajith, V.; Sobhan, C. B.; Peterson, G. P., Experimental Investigations on the Effects of Cerium Oxide Nanoparticle Fuel Additives on Biodiesel. *Advances in Mechanical Engineering* **2010**.
11. Johnson, A. C.; Park, B., Predicting contamination by the fuel additive cerium oxide engineered nanoparticles within the United Kingdom and the associated risks. *Environmental Toxicology and Chemistry* **2012,** *31*, (11), 2582-2587.
12. Karakoti, A. S.; Munusamy, P.; Hostetler, K.; Kodali, V.; Kuchibhatla, S.; Orr, G.; Pounds, J. G.; Teeguarden, J. G.; Thrall, B. D.; Baer, D. R., Preparation and characterization challenges to understanding environmental and biological impacts of ceria nanoparticles. *Surface and Interface Analysis* **2012,** *44*, (8), 882-889.
13. Deshpande, S.; Patil, S.; Kuchibhatla, S.; Seal, S., Size dependency variation in lattice parameter and valency states in nanocrystalline cerium oxide. *Applied Physics Letters* **2005,** *87*, (13).
14. Ohta, A.; Kawabe, I., REE(III) adsorption onto Mn dioxide (δ-MnO2) and Fe oxyhydroxide: Ce(III) oxidation by δ-MnO2. *Geochimica et Cosmochimica Acta* **2001,** *65*, (5), 695-703.

15. Xue, Y.; Zhai, Y. W.; Zhou, K. B.; Wang, L.; Tan, H. N.; Luan, Q. F.; Yao, X., The Vital Role of Buffer Anions in the Antioxidant Activity of CeO2 Nanoparticles. *Chemistry-a European Journal* **2012,** *18*, (35), 11115-11122.
16. Shah, V.; Shah, S.; Shah, H.; Rispoli, F. J.; McDonnell, K. T.; Workeneh, S.; Karakoti, A.; Kumar, A.; Seal, S., Antibacterial Activity of Polymer Coated Cerium Oxide Nanoparticles. *Plos One* **2012,** *7*, (10).
17. Collin, B. A., Melanie;; Johnson, Andrew; Kaur, Inder; Keller, Arturo; Lazareva, Anastasiya; Lead, Jamie; Ma, Xingmao; Merrifield, Ruth; Svendsen, Claus; White, Jason; Unrine, Jason. , Environmental release, fate and ecotoxicological effects of manufactured ceria nanomaterials. *Environmental Science: Nano* **2014,** *Accepted*
18. Auffan, M.; Rose, J.; Orsiere, T.; De Meo, M.; Thill, A.; Zeyons, O.; Proux, O.; Masion, A.; Chaurand, P.; Spalla, O.; Botta, A.; Wiesner, M. R.; Bottero, J.-Y., CeO2 nanoparticles induce DNA damage towards human dermal fibroblasts in vitro. *Nanotoxicology* **2009,** *3*, (2), 161-U115.
19. Peng, L.; He, X.; Zhang, P.; Zhang, J.; Li, Y. Y.; Zhang, J. Z.; Ma, Y. H.; Ding, Y. Y.; Wu, Z. Q.; Chai, Z. F.; Zhang, Z. Y., Comparative Pulmonary Toxicity of Two Ceria Nanoparticles with the Same Primary Size. *International Journal of Molecular Sciences* **2014,** *15*, (4), 6072-6085.
20. OECD GUIDELINES FOR THE TESTING OF CHEMICALS PROPOSAL FOR UPDATING GUIDELINE 201: Freshwater Alga and Cyanobacteria, Growth Inhibition Test. *http://www.oecd.org/chemicalsafety/testing/1946914.pdf* **2011**.
21. Baalousha, M.; Stolpe, B.; Lead, J. R., Flow field-flow fractionation for the analysis and characterization of natural colloids and manufactured nanoparticles in environmental systems: A critical review. *J. Chromatogr. A* **2011,** *1218*, (27), 4078-4103.
22. Prasad, A.; Lead, J. R.; Baalousha, M., An electron microscopy based method for the detection and quantification of nanomaterial number concentration in environmentally relevant media. *Science of the Total Environment* **2015,** *537*, 479-486.
23. Baalousha, M.; Ju-Nam, Y.; Cole, P. A.; Hriljac, J. A.; Jones, I. P.; Tyler, C. R.; Stone, V.; Fernandes, T. F.; Jepson, M. A.; Lead, J. R., Characterization of cerium oxide nanoparticles-Part 2: Nonsize measurements. *Environmental Toxicology and Chemistry* **2012,** *31*, (5), 994-1003.
24. Römer, I.; Wang, Z. W.; Merrifield, R. C.; Palmer, R. E.; Lead, J., High Resolution STEM-EELS Study of Silver Nanoparticles Exposed to Light and Humic Substances. *Environmental Science & Technology* **2016,** *50*, (5), 2183-2190.
25. Manoubi, T.; Colliex, C.; Rez, P., QUANTITATIVE ELECTRON-ENERGY LOSS SPECTROSCOPY ON M45 EDGES IN RARE-EARTH-OXIDES. *Journal of Electron Spectroscopy and Related Phenomena* **1990,** *50*, (1-2), 1-18.
26. Fortner, J. A.; Buck, E. C.; Ellison, A. J. G.; Bates, J. K., EELS analysis of redox in glasses for plutonium immobilization. *Ultramicroscopy* **1997,** *67*, (1-4), 77-81.
27. Turner, S.; Lazar, S.; Freitag, B.; Egoavil, R.; Verbeeck, J.; Put, S.; Strauven, Y.; Van Tendeloo, G., High resolution mapping of surface reduction in ceria nanoparticles. *Nanoscale* **2011,** *3*, (8), 3385-3390.
28. Yang, G.; Möbus, G.; Hand, R., Fine structure EELS analysis of glasses and glass composites. *Journal of Physics: Conference Series* **2006,** *26*, (1), 73.
29. Fabrega, J.; Zhang, R.; Renshaw, J. C.; Liu, W.-T.; Lead, J. R., Impact of silver nanoparticles on natural marine biofilm bacteria. *Chemosphere* **2011,** *85*, (6), 961-966.

30. Osborne, O. J.; Johnston, B. D.; Moger, J.; Baalousha, M.; Lead, J. R.; Kudoh, T.; Tyler, C. R., Effects of particle size and coating on nanoscale Ag and TiO2 exposure in zebrafish (Danio rerio) embryos. *Nanotoxicology* **2013,** *7*, (8), 1315-1324.
31. Hitchman, A.; Smith, G. H. S.; Ju-Nam, Y.; Sterling, M.; Lead, J. R., The effect of environmentally relevant conditions on PVP stabilised gold nanoparticles. *Chemosphere* **2013,** *90*, (2), 410-416.
32. Mirshahghassemi, S.; Cai, B.; Lead, J. R., Evaluation of polymer-coated magnetic nanoparticles for oil separation under environmentally relevant conditions: effect of ionic strength and natural organic macromolecules. *Environmental Science-Nano* **2016,** *3*, (4), 780-787.
33. Wu, L. J.; Wiesmann, H. J.; Moodenbaugh, A. R.; Klie, R. F.; Zhu, Y. M.; Welch, D. O.; Suenaga, M., Oxidation state and lattice expansion of CeO2-x nanoparticles as a function of particle size. *Physical Review B* **2004,** *69*, (12).
34. Cumberland, S. A.; Lead, J. R., Particle size distributions of silver nanoparticles at environmentally relevant conditions. *J. Chromatogr. A* **2009,** *1216*, (52), 9099-9105.
35. Dogra, Y.; Arkill, K. P.; Elgy, C.; Stolpe, B.; Lead, J.; Valsami-Jones, E.; Tyler, C. R.; Galloway, T. S., Cerium oxide nanoparticles induce oxidative stress in the sediment-dwelling amphipod Corophium volutator. *Nanotoxicology* **2016,** *10*, (4), 480-487.
36. Quik, J. T. K.; Lynch, I.; Hoecke, K. V.; Miermans, C. J. H.; Schamphelaere, K. A. C. D.; Janssen, C. R.; Dawson, K. A.; Stuart, M. A. C.; Meent, D. V. D., Effect of natural organic matter on cerium dioxide nanoparticles settling in model fresh water. *Chemosphere* **2010,** *81*, (6), 711-715.
37. Petersen, E. J.; Diamond, S. A.; Kennedy, A. J.; Goss, G. G.; Ho, K.; Lead, J.; Hanna, S. K.; Hartmann, N. B.; Hund-Rinke, K.; Mader, B.; Manier, N.; Pandard, P.; Salinas, E. R.; Sayre, P., Adapting OECD Aquatic Toxicity Tests for Use with Manufactured Nanomaterials: Key Issues and Consensus Recommendations. *Environmental Science & Technology* **2015,** *49*, (16), 9532-9547.
38. Baalousha, M.; Arkill, K. P.; Romer, I.; Palmer, R. E.; Lead, J. R., Transformations of citrate and Tween coated silver nanoparticles reacted with Na2S. *Science of the Total Environment* **2015,** *502*, 344-353.